A VISCOUS HYDRODYNAMICAL MODEL FOR RELATIVISTIC HEAVY-ION REACTIONS

By L. P. Csernai and B. Lukács

Central Research Institute for Physics, Budapest*

(Received April 29, 1983)

The dynamics of heavy ion collisions is described in a one dimensional hydrodynamical model. Numerical calculations are performed at 100 MeV/nucleon and 1 GeV/nucleon projectile energies. The density increase and the width of the shock front are evaluated for the compression stage. The differential cross section and the rapidity spectrum of the emitted nucleons are calculated.

PACS numbers: 25.70.Fg

1. Introduction

In high energy heavy ion reaction a very dense matter is produced with high energy concentration, and it seems that this is the only possibility for experimental investigation of such a state of the matter. Nevertheless, the observables of the final state do not yield direct information about the hot dense stage, between the hot stage and the observables there is the partially unknown dynamics of a very dense relativistic quantum system, and obviously first this dynamics should be treated in some way.

In the literature various approximations can be found for this dynamics, the paper of Amsden, Harlow and Nix (1977) gives a survey of them. One of these approximations is the continuum description. Since at high beam energy any solidification effect can be neglected, this description is the "(Relativistic) Fluid Dynamics" in Fig. 1 of the cited paper, and the fluid approach possesses important advantages. Namely, the relativistic fluid dynamics (within its own limitations) is a self-consistent description, it uses only a few variables, and incorporates the irreversible processes in a simple way. From technical viewpoint, the fluid description is flexible, since there is a possibility for "power expansion" with respect to the deformation velocities.

Of course, there may be some doubts about the applicability of the fluid description. For example, it requires a (more or less complete) hydrodynamical and thermodynamical local equilibrium. At the beginning of the collision such an equilibrium does not exist,

* Address: Central Research Institute for Physics, H-1525, Bp. 114, P.O.Box 49, Budapest, Hungary.

and the apparent success of cascade (Cugnon, Mizutani and Vermeulen, 1981; Knoll, 1979; Yariv and Fraenkel, 1979) and kinetic (Danielewicz, 1980; Randrup, 1979) models has risen doubts about this local equilibrium.

To achieve such an equilibrium large number of particles, sufficient time and strong interactions are necessary. The most subtle condition is the last one. The nucleons should be thermalized in a definitely shorter length than the nuclear radius. Nevertheless, it seems that the situation is not hopeless. Recent experimental studies (Tanihata, Nagamiya,

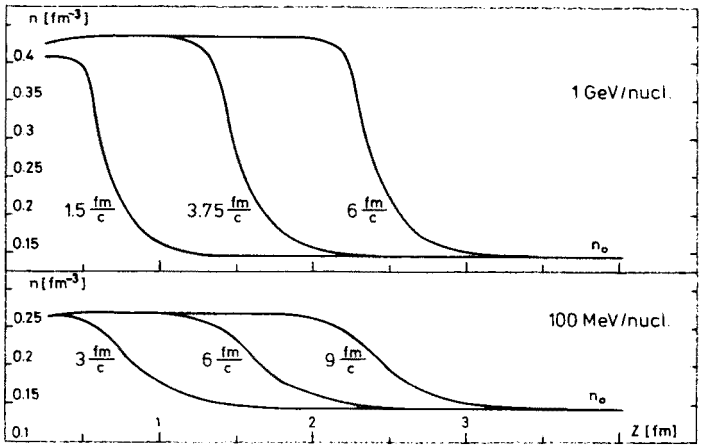

Fig. 1. Comoving density profiles of the compression shock fronts for two different projectile energies in one dimensional hydrodynamical model. Different curves belong to the indicated times

Schnetzer and Steiner, 1981) yield a value of 2.4 fm for the mean free path of a proton shot into a nucleus with high energy. It follows that for nucleus collisions the mean free path is in the order of 1 fm. If a second order phase transition occurred, the critical fluctuations might decrease the mean free path even more (Gyulassy and Greiner, 1977). The lower limit of the hydrodynamics is around 20–50 MeV/nucleon beam energy, below which the quantum effects are not negligible, and cannot be incorporated into the fluid model.

In this paper we present a simple hydrodynamical calculation for heavy ion collisions. The density and temperature increase and the width of the shock front are evaluated. We determine the differential cross section and the rapidity spectrum of the nucleons emitted at the end of the explosion.

2. *The equations of the model*

The relativistic treatment is advisable in the whole region between 50 and 1000 MeV/nucleon beam energy, although usually the relativistic corrections are proportional to $(v/c)^2$ and so these could be expected to be definitely less than 10% below 100 MeV/nucleon. However, as we shall see, the nuclear matter is a relativistic object even for low velocities.

In order to get correct dynamical equations for a relativistic system with irreversible

processes one should start from the balance equations and conservation laws. According to the fundamental idea of the general relativity, the curvature of the space-time is locally determined by the distribution of the matter. By using the principle of Occam's razor one may suppose the simplest possible equation for this relation, i.e. that the space-time curvature is represented by a two-index tensor, which does not contain higher than second derivatives, and is linear in the second order terms. Then the field equation has the form

$$R_{ik}+\lambda g_{ik} = \kappa Q_{ik} \tag{2.1}$$

where R_{ik} is the Ricci tensor formed from the metric tensor g_{ik} (Robertson and Noonan, 1969), Q_{ik} represents the distribution of the matter, while λ and κ are some constants.

By construction, both $R_{ik}-\frac{1}{2}g_{ik}R^r{}_r$ and g_{ik} are divergence-free tensors, whence

$$(Q^{ir}-\tfrac{1}{2}g^{ir}Q^s{}_s)_{;r} \equiv T^{ir}{}_{;r} = 0, \tag{2.2}$$

where the semicolon denotes covariant derivative. Eq. (2.2) leads to four conservation laws for volume integrals of some combinations of the elements of T^{ik}. Since for closed systems the energy-momentum four-vector is conserved, one must identify T^{ik} with the energy-momentum tensor, when Eq. (2.1) becomes the Einstein equation of the general relativity. Neglecting the gravitation the metric tensor becomes Minkowskian, but Eq. (2.2) survives with flat metric.

The energy-momentum tensor can be decomposed according to any timelike unit vector u_i as

$$\begin{aligned} T^{ik} &= \varrho u^i u^k + q^i u^k + q^k u^i + p^{ik}, \\ u^r u_r &= -1, \quad q^r u_r = p^{ir} u_r = 0, \end{aligned} \tag{2.3}$$

where ϱ stands for the energy density, q^i is the energy flux and p^{ik} is the stress measured by an observer moving with the four-velocity u^i (Maugin, 1974a; Maugin, 1974b; Ellis, 1971). For a fluid there is a unique velocity field in the matter, which can be chosen as u^i. Then the static part of the stress tensor has the hydrostatic form, and, stopping at the terms linear in the deformation velocity one gets:

$$p^{ik} = (p-\eta' u^r{}_{;r})(g^{ik}+u^i u^k) - \eta(u_{r;s}+u_{s;r})(g^{ir}+u^i u^r)(g^{ks}+u^k u^s) \tag{2.4}$$

where p is the pressure, while η and η' are the viscosity coefficients (Ellis, 1971; Ehlers, 1973).

According to Eq. (2.2) the divergence of T^{ik} vanishes, and we assume particle conservation too, i.e.

$$(nu^r)_{;r} = 0 \tag{2.5}$$

(n stands for the particle number density). Eqs. (2.2), (2.4–5) yield 5 equations for the 11 quantities u^i, q^i, n, p, ϱ, η and η'. Nevertheless, an equation of state connects n, ϱ and p, and some material equations express the viscous coefficients η, η', and the heat flux q^i with the thermodynamical variables and with the velocity. These additional equations determine the behaviour of the investigated type of the fluid.

The four-velocity u^i can be decomposed as

$$u^i = \frac{1}{\sqrt{1-v^2}}(\boldsymbol{v}, 1) \tag{2.6}$$

(here the units are so fixed that $c = 1$). Neglecting first all the irreversible terms and taking the limit $v \ll c$, one gets from Eqs. (2.2–4):

$$(\varrho + p)(\dot{\boldsymbol{v}} + (\boldsymbol{v}\nabla)\boldsymbol{v}) = -\nabla p \tag{2.7}$$

which is not the Euler equation; the relative correction in the density of the inertia is p/ϱ, which is 1/3 for cold relativistic Fermi gas. Using a realistic equation of state (e.g. Amsden, Harlow and Nix, 1977; Maruhn, 1977), this correction is about 10–20% for low beam energies.

Obviously, Eqs. (2.2–5) are not sufficient to calculate the dynamics of the collision; we have 5 independent equations while T^{ik} is composed of ϱ, p, u^i and q^i, by means of the two viscosity coefficients η and η', and the fifth equation contains n too. Some thermodynamical relations are necessary to establish connections among these quantities.

Since the velocity vector has three independent components, there remain only two quantities to describe the local thermodynamical state of the matter. Such a number is sufficient only in equilibrium. Nevertheless, if one assumes global equilibrium, then there are no fluxes and no irreversible processes. One consequence is that then the specific entropy remains constant along streamlines (Lukács, 1978). To demonstrate this, consider the consequence of Eq. (2.2): $T^{ir}{}_{;r}u_i = 0$. Putting $\eta = \eta' = q^i = 0$, one gets

$$\dot{\varrho} + (\varrho + p)u^r{}_{;r} = 0,$$

$$\dot{} = u^r \nabla_r. \tag{2.8}$$

Then, using the independent variables n and $\sigma = s/n$, the equilibrium relation (Ehlers, 1973; Lukács, 1978)

$$p = n\varrho_{,n} - \varrho(n, \sigma) \tag{2.9}$$

and Eq. (2.5), the result is (Landau and Lifshic, 1953)

$$\varrho_{,\sigma}\dot{\sigma} = 0. \tag{2.10}$$

So the entropy of the fluid would remain 0 during the whole process, which is of course unphysical, and the observations clearly show that the final state is not cold.

One more deficiency of the perfect fluid models is that the flow of a perfect fluid is unstable against turbulencies. In the classical regime the laminar flow is stable only if the Reynolds number $R = Lv\varrho/\eta$ is less than 1160. There does not exist such an overall condition in the whole relativistic regime, nevertheless one may assume that the critical number remains in the same range. Putting some characteristic data of a relativistic nucleus-nucleus collision into the expression of the Reynolds number, it can be seen that the critical value for η is 1–10 MeV/fm^2c.

Of course, it may be quite possible that the flow is turbulent in a collision, however, generally the calculations assume laminarity, and the numerical methods have to produce an effective "numerical viscosity" (Amsden, Harlow and Nix, 1977; Amsden, Goldhaber, Harlow and Nix, 1978). It would be more reassuring to see the effect of the true physical viscosity in the evolution of the system. Since there are some data in the literature that for normal nuclear density $\eta \simeq 6\ \mathrm{MeV/fm^2}c$ (Wieczorek, Hasse and Süssmann, 1974; Nix and Sierk, 1979), we can hope that the true process is laminar, and that there is more to gain by using viscosity than to lose in simplicity.

Of course, if there are transport fluxes in the fluid, the local equilibrium breaks down. However, there is one convenient limiting situation: if the fluxes are small in first order, then the deviations from the local equilibrium are of second order (Ehlers, 1973). So an equilibrium treatment with fluxes can have some physical meaning, there exist situations when the fluxes are too weak to destroy the local equilibrium. Of course, it is not too easy to check the validity of this approximation, since the momentum distributions are not explicitly used in this description. One may guess that the local states evolve through more or less equilibrium states if $\dot{\sigma} < 1/\tau$ where τ is some characteristic time of the interactions, i.e. when the changes in the momentum distributions can in fact be produced by the actual interactions (because the change rate of the specific entropy is characteristic for the velocity of the evolution of the momentum distribution). The unequality seems to be valid for the present case.

For local equilibrium the local data are determined by the particle density n and by one thermal data, i.e. by σ. The form of the energy density function $\varrho = \varrho(n, \sigma)$ has to be fixed, and then the other local data can be calculated, for example p is expressed through Eq. (2.9).

The laws of the fluxes have to be fixed too. In Eq. (2.4) we accepted a linear form for the momentum transport; there exists a linear approximation for the heat transport too (Ehlers, 1973; Maugin, 1974a). Then there remain three transport coefficients to determine; they depend on n and σ.

Since we want to keep the viscosity in the calculation, the computation would become technically too complicated. Thus here we restrict ourselves to a one dimensional hydrodynamics. Then there is no difference between the shear and bulk viscosities. For the only viscosity coefficient one can expect at least temperature dependence, which occurs even in the simplest models (Kennard, 1938). Here we accept the function yielded by the first approximation for Fermi gases (Huang, 1963; Galitskii, Ivanov and Khangulyan, 1979):

$$\eta \simeq \tfrac{1}{3}\varrho\lambda\langle v_{\mathrm{th}}\rangle \simeq (8\sigma_{\mathrm{tot}})^{-1}\sqrt{m(T_0+T)}\,,$$

$$T_0 = \frac{9}{16mc^2}(3\pi^2/2)^{2/3}n^{2/3}(\hbar c)^2. \tag{2.11}$$

Since the heat conductivity is not so crucial for the stability and the final state as the viscosity, we neglect it from technical reasons. Finally, we choose the same function for the energy density as Amsden, Harlow and Nix (1977). This equation of state has the same heat term as the nonrelativistic Fermi gas in the T^2 approximation.

Eqs. (2.2–5) lead to the following balances:

$$\mathring{N} = -N \operatorname{div} \boldsymbol{v},$$

$$\mathring{\boldsymbol{M}} = -\boldsymbol{M} \operatorname{div} \boldsymbol{v} - \operatorname{grad} \Pi,$$

$$\mathring{E} = -E \operatorname{div} \boldsymbol{v} - \operatorname{div} (\Pi \boldsymbol{v}), \tag{2.12}$$

where

$$\circ = \partial_t + \boldsymbol{v} \operatorname{grad}, \tag{2.13}$$

and

$$N = \frac{n}{\sqrt{1-v^2}},$$

$$M^\alpha = T^{0\alpha} = (\varrho + \Pi) \frac{v^\alpha}{1-v^2},$$

$$E = T^{00} = \frac{\varrho + \Pi v^2}{1-v^2},$$

$$\Pi = p + \eta' \frac{\mathring{n}}{n\sqrt{1-v^2}}. \tag{2.14}$$

The balance equations (2.12) completely determine the evolutions of the independent variables $\boldsymbol{v}$, n and σ (of course, in our case $v_x = v_y = 0$). Nevertheless it is convenient to get an equation directly to σ. Starting again from $T^{ir}{}_{;r} u_i = 0$, the result is as follows:

$$\mathring{\sigma} = \frac{\eta' \mathring{n}^2}{n^3 T \sqrt{1-v^2}}. \tag{2.15}$$

Of course, this equation is not independent of the system (2.12). The details of the integration of the balance equations can be found in the Appendix. (See also: Csernai, Lukács and Zimányi, 1980).

3. The hydrodynamical stage

In the one dimensional model two slabs of nuclear matter are stopped and compressed. In the beam (z) direction the initial lengths of the slabs are chosen the same as the diameters of the colliding nuclei; here we restrict ourselves to U+U and Ca+Ca reactions.

Fig. 1 shows density profiles at different stages of the compression for two characteristic beam energies. The profiles are similar to shock fronts, however, they are not sharp; their widths are around 1 fm. (If the temperature and density dependence of the viscosity coefficient were neglected, the width would be 0.2–0.5 fm.) Such a width seems quite reasonable.

After the maximal compression there is a hydrodynamical expansion. Although the initial and final geometries are similar, the whole process is not symmetric in time,

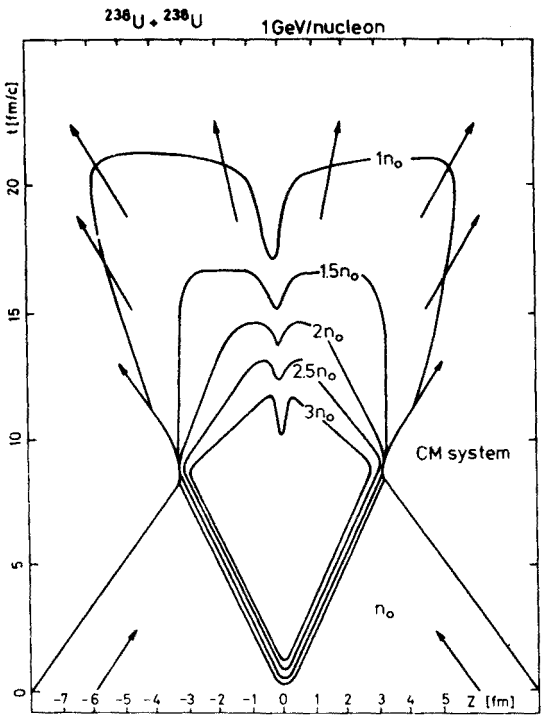

Fig. 2. Distribution of comoving density in space and time for a U+U collision at 1 GeV/nucleon projectile energy. The arrows represent the motion of the fluid elements

because of the entropy production. Fig. 2 shows the distribution of the density in space and time. It can be seen that the location of the density increase practically does not accelerate during the compression stage, as in stationary shock approximations.

4. Calculations of the cross section

The hydrodynamical description of the expansion breaks down at some density. E.g. reaching a $p < 0$ state, the matter becomes unstable against microscopic collapse (Harrison, Thorne, Wakano and Wheeler, 1965), leading to a cluster of droplets. The result is similar if the mean distance of the particles becomes too great, and thus the interactions become negligible. In our model the continuous decay of the collective state is substituted by a sudden break-up. The nuclear matter is assumed to flow in a "tube", but when the fluid cells at the two edges of the matter reach $n = 0.75n_0$ or $p = 0$, the constraint caused by the tube vanishes and the cells explode into all directions due to the thermal velocities of the nucleons. Thus this final part of the calculation is three-dimensional.

The thermal distribution of the nucleons inside a fluid cell i is described by the relativistic Fermi distribution:

$$f_i(\boldsymbol{p})d^3p = \frac{4}{(2\pi\hbar)^3}\{\exp[(\sqrt{m^2+\boldsymbol{p}^2}-\mu_i)/T_i]+1\}^{-1}d^3p \tag{4.1}$$

where μ_i is the chemical potential taken from the normalization condition

$$n_i = \frac{4}{(2\pi\hbar)^3}\int f_i(\boldsymbol{p})d^3p. \tag{4.2}$$

To obtain the momentum distribution of all nucleons in one definite reference frame the distributions (4.1) are to be Lorentz-transformed to this frame (denoted by Lab) by the relative boost velocity $\boldsymbol{\beta}_i$ of the cell i:

$$f_i^{\mathrm{Lab}}(\boldsymbol{P})d^3\boldsymbol{P} = \frac{w(\boldsymbol{P})}{W} f_i(\boldsymbol{p}(\boldsymbol{P}))d^3P, \tag{4.3}$$

where $(w, \boldsymbol{p})$ and $(W, \boldsymbol{P})$ are the four-momenta in the cell and Lab systems, respectively. They are connected by Lorentz-transformations:

$$w = \gamma W - \gamma\boldsymbol{\beta}\boldsymbol{P}$$

$$\boldsymbol{p} = \boldsymbol{P} - \boldsymbol{\beta}\gamma\frac{w+W}{\gamma+1}; \quad \gamma = \frac{1}{\sqrt{1-\beta^2}}. \tag{4.4}$$

In the present one-dimensional hydrodynamics the scalar product $\boldsymbol{\beta}_i\boldsymbol{P} = \beta_i\sqrt{W^2-m^2}\cos\theta$ due to the fact that all cells move along the z axis. Thus from Eqs. (4.3–4) we obtain the following double differential distribution of the nucleons:

$$g(W, \theta)dWd\Omega = \sum_i \mathrm{Vol}_i \frac{4}{(2\pi\hbar)^3}\frac{A_i\sqrt{W^2-m^2}\,dWd\Omega}{\exp\left[(A_i-\mu_i)/T_i\right]+1} \tag{4.5}$$

where Vol_i is the volume of the i^{th} cell, and

$$A_i = \gamma_i(W - \beta_i\sqrt{W^2-m^2}\cos\theta). \tag{4.6}$$

In the general case when the flow is three-dimensional, the distribution (4.5) remains valid, but $A_i = \gamma_i(W-(\boldsymbol{\beta}_i\boldsymbol{P}))$.

5. *Calculation of rapidity spectra*

The rapidity spectrum is convenient to describe the cross section both in Lab and in CM systems in the same time. It can be expressed from the distributions (4.1) and (4.5). Let us start by the definition of the rapidity:

$$y_\parallel = \tfrac{1}{2}\ln\frac{w+p_\parallel}{w-p_\parallel} = \tfrac{1}{2}\ln\frac{1+\beta_\parallel}{1-\beta_\parallel} = \mathrm{arth}\,\beta_\parallel,$$

$$\boldsymbol{y}_\perp = (y_\perp, \phi) = \frac{1}{m}\boldsymbol{p}_\perp = \gamma\boldsymbol{\beta}_\perp. \tag{5.1}$$

The inverse transformation is:

$$p_\perp = m y_\perp,$$

$$p_\parallel = m\sqrt{1+y_\perp^2}\sinh(y_\parallel),$$

$$w = m\sqrt{1+y_\perp^2}\cosh(y_\parallel). \tag{5.2}$$

Using these definitions, the rapidity distribution

$$f'(y_\parallel, y_\perp, \phi)dy_\parallel dy_\perp d\phi = f(\boldsymbol{p})d^3p = f(\boldsymbol{p})p_\perp dp_\parallel dp_\perp d\phi \tag{5.3}$$

of the i^{th} cell is, according to Eq. (4.1):

$$f_i'(y) = \frac{4}{(2\pi\hbar)^3}\,\frac{m^3 y_\perp\sqrt{1+y_\perp^2}\cosh(y_\parallel)}{\exp\left[(m\sqrt{1+y_\perp^2}\cosh(y_\parallel)-\mu_i)/T_i\right]+1}. \tag{5.4}$$

Due to the additivity of $y_{||}$, the total Lab distribution is:

$$g'(Y_\parallel, Y_\perp)dY_\parallel dY_\perp d\phi = \sum_i \mathrm{Vol}_i f_i'(Y_\parallel - Y_\parallel^i, Y_\perp)dY_\parallel dY_\perp d\phi, \tag{5.5}$$

where $Y_{||}^i$ is the rapidity of the i^{th} cell in the Lab frame, $Y_{||}^i = \operatorname{arth}\beta_i$. (Note that this result is valid only for one dimensional flow, since otherwise the rapidity is not additives.) In the general case the rapidity spectrum can be expressed as

$$g'(Y_\parallel, Y_\perp)dY_\parallel dY_\perp d\phi = \sum_i \mathrm{Vol}_i \frac{4}{(2\pi\hbar)^3}\,\frac{m^2 Y_\perp B_i dY_\parallel dY_\perp d\phi}{\exp\left[(B_i-\mu_i)/T_i\right]+1}$$

$$B_i = m\gamma_i\left[\sqrt{1+Y_\perp^2}\,(\cosh(Y_\parallel)-\beta_{i\parallel}\sinh(Y_\parallel))-(\boldsymbol{\beta}_{i\perp}Y_\perp)\right] \tag{5.6}$$

which reduces to (5.5) in the above special case.

6. The effect of dynamics on the measurable quantities

One expects that in the compression stage the viscosity does not affect much the resulting values of the density and temperature, because as long as the flow remains stationary, the shock front formalism yields the same increase (Flügge, 1959), and η affects only the width of the front. Of course, for finite nuclei the flow cannot be exactly stationary, nevertheless, the lower part of Fig. 2 shows the approximate stationarity of the motion of the front during the compression.

This is not true in the expansion stage, so this phase is already more sensitive to the viscosity, and a shock front approximation is not sufficient.

The equation of state used in the present calculation has been taken from the paper of Amsden, Harlow and Nix (1977). Of course, the final cross section depends on the equation of state (and specially, this dependence can be strong when phase transitions are taken into account).

In this paper, from technical reasons, we restricted ourselves to collinear flow. This model has the advantage that the time evolution of the system is simple, it can be clearly

divided into two essentially different phases, as it is seen on Fig. 2. Nevertheless, it causes the unphysical result that only the forward angles are affected by the flow. This obviously leads to an essential difference from the results of Amsden, Harlow and Nix (1977) or of Danielewicz (1979).

When the full compression is reached, the incident energy of the projectile has been transformed into the thermal and compression energy of the dense nuclear matter which is approximately at rest in the CM frame. Both the thermal and the compression energy provide pressure that starts to push out the nuclear matter from the center. Thus the energy is transformed into the kinetic energy of the hydrodynamic energy of the flow and the temperature decreases almost adiabatically in the expansion (Stöcker, Maruhn and Greiner, 1979). The slightly lower density of the center (see Fig. 2) is inherited from the compression phase: Fig. 1 shows that there is a slight density decrease in the center, and in the same time the temperature is higher to produce sufficient pressure there. Since the heat transfer is neglected in our calculation, the central temperature excess cannot diminish during the collision process and then the pressure balance conserves the central density decrease. On the other hand, the central density depression of the compression phase can be traced back until the initial condition at the edges of the slabs to avoid infinite gradients (see the Appendix). Thus this depression is an artifact of the model. Nevertheless, the depression is relatively slight, and it affects only a small portion of the total volume, so the problem does not seem to be serious.

Obviously our breakup model is an approximation only. Although the addition of

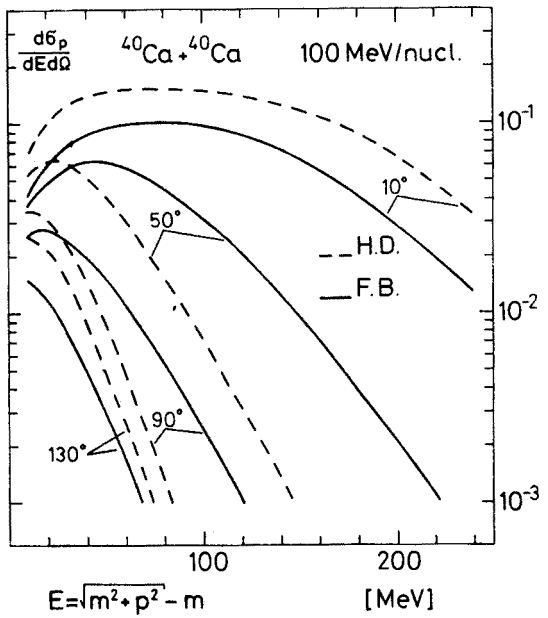

Fig. 3. Double differential cross sections $d\sigma/dEd\Omega$ for the inclusive primary charged spectrum (Gyulassy, 1979) of a $^{40}Ca + {}^{40}Ca$ collision at 100 MeV/nucleon projectile energy. The full curves represent the results of the one dimensional model; the dashed ones belong to the "fireball" model

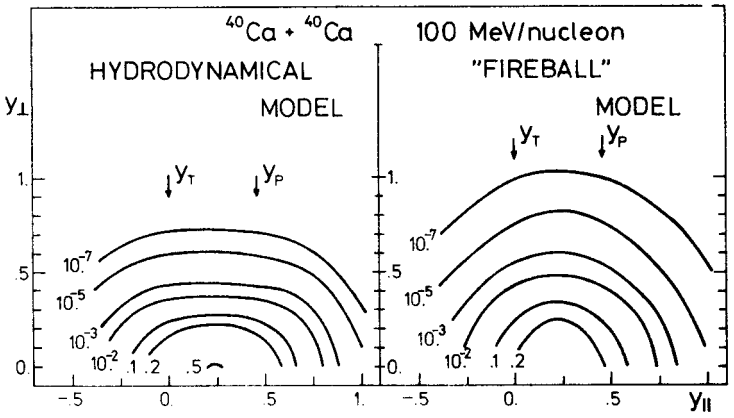

Fig. 4. Contour plots of rapidity distribution $g/Y_\perp$ for $^{40}Ca + ^{40}Ca$ collision at 100 MeV/nucleon projectile energy (arbitrary units)

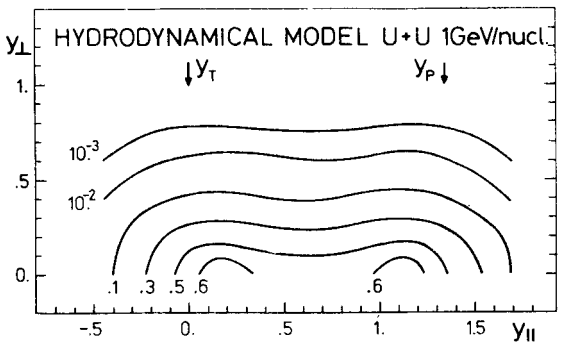

Fig. 5. Contour plots of rapidity distribution $g/Y_\perp$ for the inclusive primary charged spectrum of a U + U collision at 1 GeV/nucleon projectile energy (arbitrary units)

the hydrodynamical and thermal momenta is correct, one might choose different breakup conditions too, and the breakup condition can seriously affect the final spectra.

To demonstrate the effect of various breakup conditions, in some calculations we set the breakup at the end of the compression phase (although this is an unphysical condition, because the nucleon-nucleon interactions cannot become negligible at the maximal density). Then the model becomes similar to fireball ones, because there is no flow at the final stage. The results of this modified model are referred as "Fireball" later.

In Fig. 3 the primary charged inclusive spectra (Gyulassy, 1979) are plotted for a one dimensional $^{40}Ca + ^{40}Ca$ collision in the hydrodynamical and fireball model. There are essential differences in the differential cross sections. In forward (10°) and backward (130°) directions the linear hydrodynamical model gives higher cross sections, while in transverse directions the "fireball" model produces greater yield apart from very low (10–20 MeV) energies. The inclusive charged primary rapidity spectrum (Fig. 4) furnishes a better means to show the reason for the differences. The "fireball" model shows an isotropic momentum distribution in the CM frame due to the fact that the fluid cells are not moving at the

breakup. The spectrum of the "hydrodynamic" model is also symmetric in CM, but it is elongated in the beam direction, because the compression energy has been transformed into the kinetic energy of the one dimensional flow. In real, three-dimensional collisions there might be various possibilities:

a) The hydrodynamical flow may be isotropic. Then the distinction between "fireball" and "hydrodynamical" models can be seen only by comparing the energy dependences (Siemens and Rasmussen, 1979).

b) At high energies (several GeV/nucleon) and for relatively soft equation of state the one dimensional nature of the flow should dominate, i.e. the major part of the compression energy should appear in the beam direction. At higher energies the rapidity spectrum might show more elongated shape as the compression energy plays a more essential role (Fig. 5).

c) At beam energies below 1 GeV/nucleon and for hard equations of state the major part of the compression energy is transformed into transversal directions (let us remind the flow of incompressible water). In this case the rapidity spectrum of central symmetric

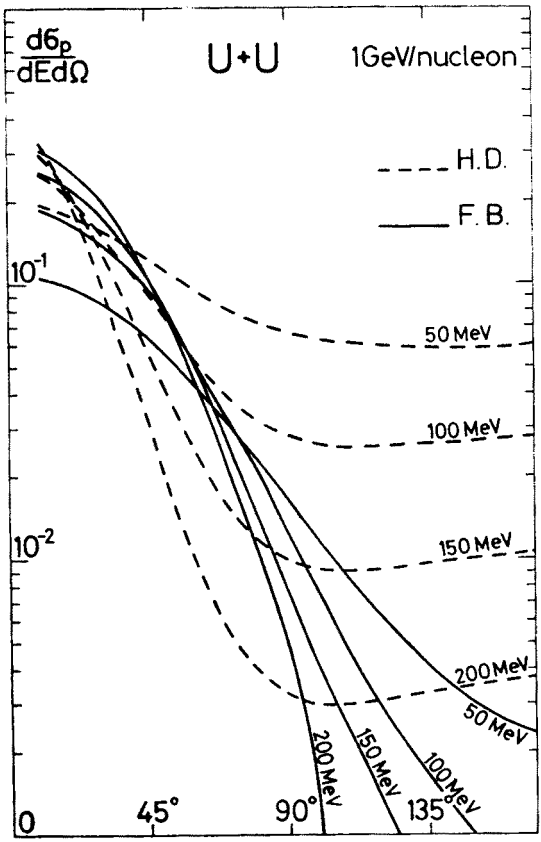

Fig. 6. Double differential cross section $d\sigma/dEd\Omega$ for the inclusive primary charged spectrum of a U + U reaction at 1 GeV/nucleon projectile energy. The full curves represent the one dimensional hydrodynamical model, the dashed ones belong to the "fireball" version

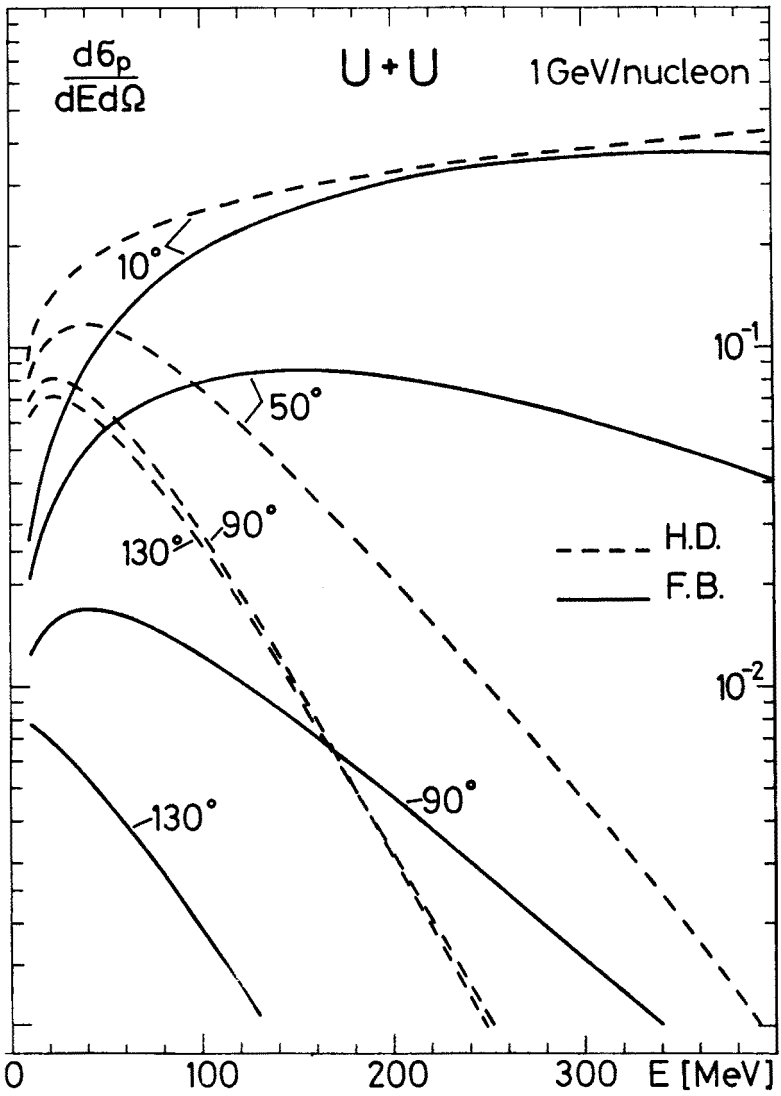

Fig. 7. Polar angle (θ) dependence of the double differential cross section $d\sigma/dEd\Omega$ for the inclusive primary charged spectrum of a U + U reaction at 1 GeV/nucleon projectile energy

collisions should show a deviation from the isotropic "fireball" spectrum, and the transversal directions should bear higher yield (Amsden, Harlow and Nix, 1977; Stöcker et al., 1982). Our one dimensional model cannot reproduce this behaviour.

In Fig. 5 the rapidity spectrum of a 1 GeV/nucleon U+U collision is plotted, which is more elongated than at 100 MeV/nucleon (Fig. 4). The difference between the hydrodynamical and "fireball" models is striking on the double differential cross section (Fig. 6) specially when it is plotted versus the angles and parametrized by the energy (Fig. 7). In this figure one can see that the difference appears in the backward angles strikingly.

7. *Conclusions*

This paper furnishes barely a model study of possibilities. Direct comparison to experimental results would not be too reasonable, because in more extended three-dimensional calculations such comparisons were already made (Amsden, Harlow and Nix, 1977; Amsden, Goldhaber, Harlow and Nix, 1978; Stöcker et al., 1981; Stöcker et al., 1982).

However, such simpler studies provide a deeper insight into details and might contribute to the recognition of some elementary basic collective processes. As an example we mention only the elongated rapidity distribution (Fig. 5), which is qualitatively observed in experiments too. Although this effect is caused mainly by the spectator evaporation in noncentral collisions and/or possibly by some transparency of the nuclei, our results show that hydrodynamical models can reproduce such an effect for soft equations of state without assuming the previous two processes. It is also very enlighting that by the variation of the breakup condition the resulting spectra vary considerably, thus showing us that this final breakup process is of great importance in determining the observables.

The central nonsymmetric collisions, which can also be described approximately by one dimensional hydrodynamical models, are discussed elsewhere (Csernai and Fái, 1983).

APPENDIX

The method of the numerical integration

Let us collect the system of equations to be solved:

$$\dot{N} = -Nv_{,z}, \tag{A.1a}$$

$$\dot{M} = -Mv_{,z} - \Pi_{,z}, \tag{A.1b}$$

$$\mathring{\sigma} = \eta' \mathring{n}^2/(n^3 T\sqrt{1-v^2}), \tag{A.1c}$$

$$^{\circ} = \partial_t + v\partial_z, \tag{A.2}$$

$$N = n(1-v^2)^{-1/2}, \tag{A.3a}$$

$$M = (\varrho + \Pi)v(1-v^2)^{-1}, \tag{A.3b}$$

$$\Pi = p + \eta' \mathring{n}/(n\sqrt{1-v^2}), \tag{A.3c}$$

$$\varrho = \varrho(\sigma, n) \text{ is a given function,} \tag{A.4a}$$

$$p = p(\sigma, n) \text{ is a given function,} \tag{A.4b}$$

$$T = T(\sigma, n) \text{ is a given function,} \tag{A.4c}$$

$$\eta' = \eta'(\sigma, n) \text{ is a given function.} \tag{A.4d}$$

From $t = 0$ the equation

$$\dot{E} = -Ev_{,z} - (\Pi v)_{,z} \tag{A.5}$$

was solved simultaneously and the value of $E(z, t)$ obtained in this way was compared to

$$\tilde{E} = (\varrho + \Pi v^2)(1 - v^2)^{-1}. \tag{A.6}$$

A Lagrangian method was used for solving the system of equations. The fluid was divided into N_p (one dimensional) cells. The length of each cell was $\Delta z = 0.2 r_0$ at $t = 0$. For the initial moment the fluid was described as two slabs moving toward each other and just touching each other at $z = 0$. The process is described in the CM system, thus the position of the fluid element at $z = 0$ is fixed during the whole process. All the fluid elements $i = 1, \ldots, N_p$ are characterized by their positions z, i, t and by the parameters: N, M, σ, n, v, ϱ, p, η', Π, T, E, $\tilde{E}$ and by the derivatives $\Pi_{,z}$, $v_{,z}$ and $\dot{n}$. The system of equations is of implicitly second order, because in Eq. (A.1b) Π contains $\dot{n}$. However, we took the term containing $\dot{n}$ in Π as perturbation and solved the system of equations in the following way:

At $t = 0$ the parameters z, N, M, σ, n, v, ϱ, p, Π, T, η', E, $\tilde{E}$ were given for each cell together with $\Pi_{,z}$, $v_{,z}$, $\dot{n}$ (according to the initial conditions that there were two just touching homogeneous nuclei moving rigidly). The parameters obeyed the equations (A.3–4) and $\tilde{E} = E$ was fulfilled.

At the time t the evolution of the parameters was calculated by

$$z(i, t+\Delta t) = z(i, t) + v(i, t)\Delta t, \tag{A.7}$$

$$N(i, t+\Delta t) = N(i, t) - N(i, t) v_{,z}(i, t)\Delta t, \tag{A.8}$$

$$M(i, t+\Delta t) = M(i, t) - M(i, t) v_{,z}(i, t)\Delta t - \Pi_{,z}(i, t)\Delta t, \tag{A.9}$$

$$\sigma(i, t+\Delta t) = \sigma(i, t) + \eta'(i, t)\dot{n}(i, t)^2 / [n(i, t)^3 T(i, t) \sqrt{1 - v(i, t)^2}]. \tag{A.10}$$

The time step was chosen to be $\Delta t = 0.01$–0.08 fm/c depending on the projectile energy. From Eqs. (A.3) the following relation can be derived:

$$M = (\varrho + p + \eta' N n / n^2) N^2 (1 - n^2/N^2)^{1/2} / n^2. \tag{A.11}$$

This equation was solved to get $n(i, t+\Delta t)$ using M, N and σ in $t+\Delta t$, together with ϱ, p and η' (functions of the unknown n and the known σ) and taking $\dot{n}$ from the previous time step.

Having obtained n and using the equation of state p and T can be calculated, Eq. (A.4d) yields η', while the velocity can be obtained from Eq. (A.3a) as

$$v(i, t+\Delta t) = \sqrt{1 - \frac{n(i, t+\Delta t)^2}{N(i, t+\Delta t)^2}}\ \mathrm{Sign}\,(M). \tag{A.12}$$

Now we can correct $\dot{n}$ as

$$\dot{n}(i, t+\Delta t) = 0.5[n(i, t+\Delta t) - n(i, t-\Delta t)]/\Delta t. \tag{A.13}$$

Then using Eq. (A.3c) $\Pi(i, t+\Delta t)$ is determined. The derivatives $\Pi_{,z}(i, t+\Delta t)$ and $v_{,z}(i, t+\Delta t)$ were determined from first order formulae and then averaged over a range of 3–5 cells.

The first and last values of $\Pi_{,z}$ were calculated as

$$\Pi_{,z}(1, t) = \frac{\Pi(1)-0.0}{z(2)-z(1)}.$$

$$\Pi_{,z}(N_p, t) = \frac{0.0-\Pi(N_p)}{z(N_p)-z(N_p-1)}. \tag{A.14}$$

Having obtained $z, N, M, \sigma, n, v, \varrho, p, \eta', T$ and Π at $t+\Delta t$, $\tilde{E}(i, t+\Delta t)$ is given through Eq. (A.6). Using the differential equation (A.5) the quantity E can be obtained as

$$E(i, t+\Delta t) = E(i, t)\,(1-v_{,z}(i, t)\Delta t)-\Pi(i, t)v_{,z}(i, t)\Delta t-v(i, t)\Pi_{,z}(i, t)\Delta t. \tag{A.15}$$

Then the relative difference of $\tilde{E}$ and E can be evaluated, which would be 0 if we had the correct solution. Thus $\tilde{E}-E/E$ is a quantity measuring the quality of the integration.

REFERENCES

Amsden, A. A., Harlow, F. H., Nix, J. R., *Phys. Rev.* **C15**, 2059 (1977).

Amsden, A. A., Goldhaber, A. S., Harlow, F. H., Nix, J. R., *Phys. Rev.* **C17**, 2080 (1978).

Csernai, L. P., Fái Gy., *Acta Phys. Hung.* (1983) in press.

Csernai, L. P., Lukács, B., Zimányi, J., *Lett. Nuovo Cimento* **27**, 111 (1980).

Cugnon, J., Mizutani, T., Vermeulen, J., *Nucl. Phys.* **A352**, 505 (1981).

Danielewicz, P., *Nucl. Phys.* **A314**, 465 (1979).

Danielewicz, P., Proc. Int. Conf. Extr. States in Nucl. Syst., Dresden 1980.

Ehlers, J., in *Relativity, Astrophysics and Cosmology*, ed. W. Israel, D. Reidel Publ. Comp., Dordrecht-Boston 1973, p. 1.

Ellis, G. F. R., *Proc. Int. School Phys. "Enrico Fermi"* **47**, 104 (1971).

Flügge, S., *Handbuch der Physik*, Vol. 8/1, Berlin-Göttingen-Heidelberg 1959, p. 226.

Galitskii, V. M., Ivanov, Yu. B., Khangulyan, V. A., *Yad. Fiz.* **30**, 778 (1979).

Gyulassy, M., Proc. EPS Top. Conf. Large Ampl. Coll. Nucl. Motions, Keszthely 1979.

Gyulassy, M., Greiner, W., *Ann. Phys.* **109**, 485 (1977).

Harrison, B. K., Thorne, K. S., Wakano, M. Wheeler, J. A., *Gravitation Theory and Gravitational Collapse*, Univ. Chicago Press 1965.

Huang, K., *Statistical Mechanics*, Wiley, New York-London 1963.

Kennard, E. H., *Kinetic Theory of Gases*, McGraw-Hill, N. Y. 1938.

Knoll, J., *Phys. Rev.* **C20**, 773 (1979).

Landau, L. D., Lifshic, E. M., *Teoreticheskaya fizika VI. Gidrodinamika* (1953).

Lukács, B., KFKI-1978-82 (1978).

Maruhn, J. A., Proc. Top. Conf. Heavy Ion Coll. Fall Creek Falls, State Park Tenessee, 1977, p. 156.

Maugin, G. A., *J. Phys. A* **7**, 465 (1974a).

Maugin, G. A., *Gen. Relativ. Gravitation* **5**, 13 (1974b).

Nix, J. R., Sierk, A. J., LA-UR-79-1632 (1979).

Randrup, J., *Nucl. Phys.* **A314**, 429 (1979).

Robertson, H. P., Noonan, T. W., *Relativity and Cosmology*, W. B. Saunders, Philadelphia 1969.

Siemens, P. J., Rasmussen, J. O., *Phys. Rev. Lett.* **42**, 880 (1979).

Stöcker, et al., *Phys. Rev. Lett.* **47**, 1807 (1981).
Stöcker, et al., *Phys. Rev.* **C25**, 1873 (1982).
Stöcker, H., Maruhn, J., Greiner, W., *Phys. Lett.* **81B**, 303 (1979).
Tanihata, I., Nagamiya, S., Schnetzer, S., Steiner, H., *Phys. Lett.* **100B**, 121 (1981).
Wieczorek, R., Hasse, R. W., Süssmann, G., *Physics and Chemistry of Fission*, I.A.E.A. Vienna 1974, Vol. I, p. 523.
Yariv, Y., Fraenkel, Z., *Phys. Rev.* **C20**, 2227 (1979).